Tasmania

Mineral Resources Tasmania
Report 1993/26

Blue amphibole in the Proterozoic to Cambrian Arthur Metamorphic Complex, northwest Tasmania

by N. J. Turner and R. S. Bottrill

CONTENTS

TABLES

FIGURES

Introduction

Blue amphibole minerals have long been known to occur in the Whyte Schist near the site of what is now the Reece Dam (Spry, 1964) and at the Savage River mine (Spiller, 1974). Recently published mapping (Turner *et al*., 1991) has shown that these two localities are within the same rock unit called the Bowry Formation (fig. 1). The recent mapping has also identified several additional localities in the Bowry Formation where blue amphibole occurs but no occurrences were found in the Arthur Metamorphic Complex outside the Bowry Formation.

This report describes the new occurrences of blue amphibole and shows that the mineralogy and texture of the host rocks range from an unusual, little altered prograde assemblage in massive amphibolite, through partially retrogressed assemblages in foliated amphibolite, to a strongly retrogressed assemblage in mafic schist. The compositions of the blue amphibole minerals and of some host amphibolites have been determined, and the significance of these data are discussed. Comparison is also made between the Arthur Metamorphic Complex and the similar Japanese Sambagawa Belt (Wallis and Banno, 1990).

Setting

The Arthur Metamorphic Complex comprises pelitic, dolomitic and quartzose schist with interbanded amphibolite derived from tholeiitic volcanic rocks and related intrusive rocks. Most rocks in the complex are of greenschist facies, although relict blueschist and possibly amphibolite facies minerals are preserved in the Bowry Formation (fig. 1).

The metamorphic complex corresponds to a narrow tectonic feature known as the Arthur Lineament (Gee, 1967) which transects northwest Tasmania from Ahrberg Bay on the west coast to near Wynyard on the north coast, a distance of about 110 kilometres. The complex has a maximum width of about 10 km and is at its most varied in the Corinna district (Turner *et al*., 1991), where it has previously been called the Whyte Schist (Spry, 1964).

Near the north coast the Arthur Metamorphic Complex is transitional along its western boundary with less deformed and relatively unmetamorphosed rocks of the Rocky Cape Group (Gee, 1989). The eastern boundary at the north coast is obscured but in the south, near Corinna, the eastern boundary is a transition from metamorphosed Oonah Formation to relatively unmetamorphosed Oonah Formation (fig. 1).

A fault forms the western boundary of the complex near Corinna. This fault marks the western edge of the Whyte Schist, not the western edge of metamorphism. Across the fault there is a reduction in degree of metamorphic recrystallisation from schist and amphibolite of usually medium grain size in the Arthur Metamorphic Complex to slate and fine-grained greenschist-facies metabasalt in the Ahrberg Group. The lower grade of metamorphism persists westward into rocks similar to the Rocky Cape Group but which are not necessarily direct correlates of that unit.

The overall stratigraphic and structural relationships in the Corinna district are a matter of some conjecture. Brown (1986) considered that most deformation in the Oonah Formation, and by implication, in the Arthur Metamorphic Complex and Ahrberg Group, occurred before the Success Creek Group and Crimson Creek Formation (fig. 1) were deposited. Turner *et al*. (1992) considered it likely that the basaltic rocks in the metamorphic complex and Ahrberg Group are equivalent to the relatively undeformed and unmetamorphosed basalts in the Crimson Creek Formation. Such a relationship requires that the deformation and metamorphism in the complex be younger than the probable Late Proterozoic depositional age of the Crimson Creek Formation. A strong indication of a younger age is provided by Early Palaeozoic K-Ar metamorphic ages of 494–510 Ma derived from green amphibole in the Bowry Formation (Turner *et al*., 1992; Turner, 1993).

Previous work on blue amphibole in the district

Blue amphibole was first described from rocks belonging to the Bowry Formation by Spry (1964), who identified 60% by volume of glaucophane in amphibolite south of the Stringer Creek–Pieman River junction, close to the present Reece Dam. Crossite was given as a supplementary (?varietal) name for this amphibole. It should be noted here that crossite is no longer a valid name for intermediate members of the glaucophane-magnesioriebeckite series, which are now described according to their major end-member (Leake *et al*., 1997). The remainder of the mineral assemblage in the amphibolite comprised abundant epidote and albite with accessory sphene, apatite, magnetite, muscovite, tourmaline and chlorite. Major element analysis of the amphibolite showed a soda-rich, basic composition.

Other petrological work was carried out near the Stringer Creek–Pieman River junction by the Hydro-Electric Commission during dam site investigations. Blue amphibole was identified in a number of samples taken from diamond-drill core. The investigations are described in unpublished HEC reports.

Green and Spiller (1977) and Spiller (1974) described blue amphiboles from the Savage River mine, where the mineral occurs in metabasalt and mafic schist. The mineral assemblages in which the blue amphiboles are present are variable but most assemblages contain actinolite, albite, epidote, chlorite and quartz. They are not equilibrium assemblages and the blue amphibole grains are always rimmed by actinolite. Chemically, the most sodic blue amphibole composition identified

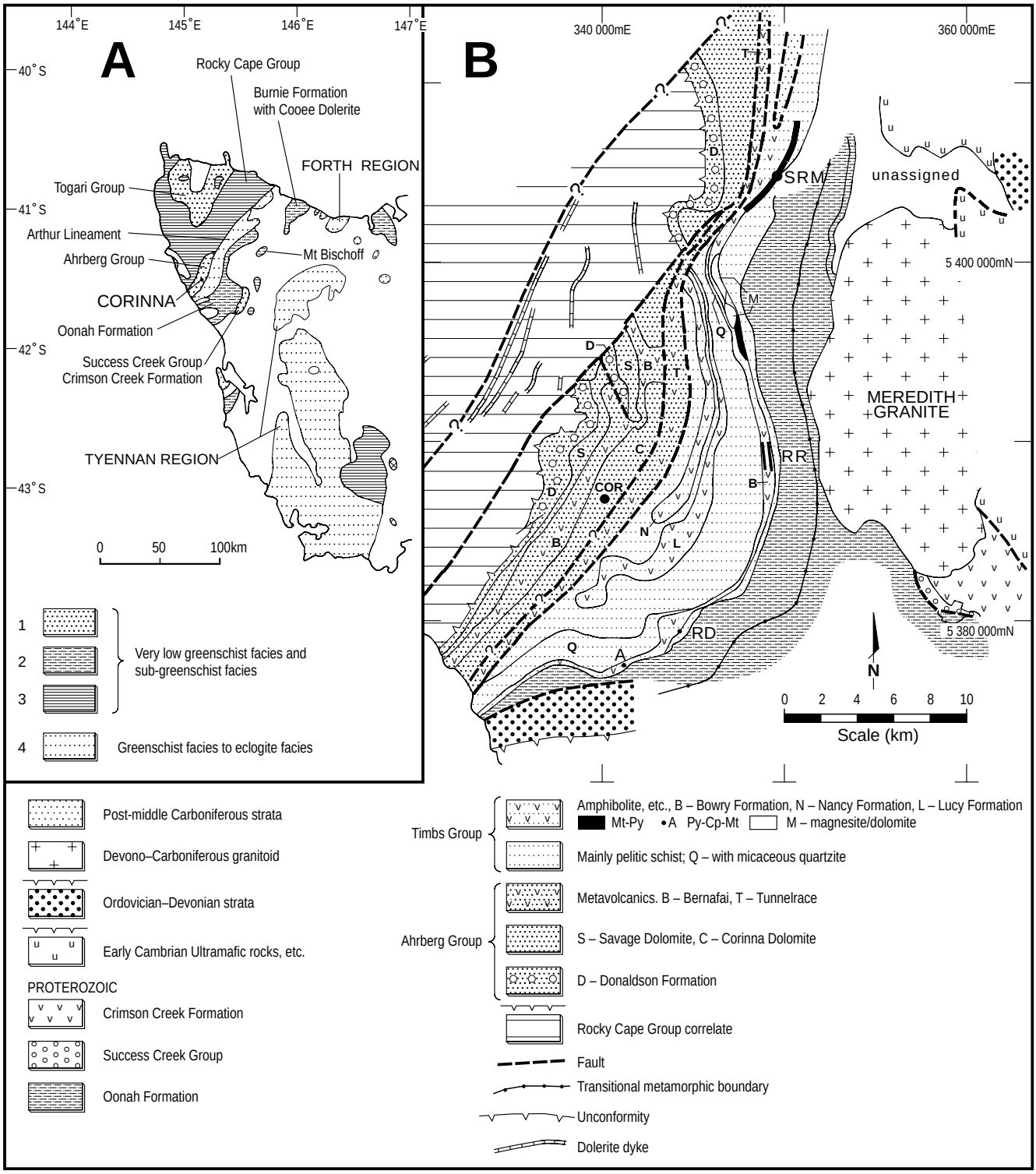

Figure 1

A — Western Tasmania showing the Proterozoic rocks (1, 2, 3) and c.510–515 Ma metamorphic rocks (4) derived from Proterozoic rocks.
1 – continental shelf and margin deposits with rift tholeiites near the top;
2 – sandy turbidite; 3 – quartz arenite, siltstone, minor dolomite;
4 – Forth and Tyennan regions largely similar to 3. Note: very low greenschist = chlorite zone.

B — Geology of the Corinna district after Turner et al. *(1991). The Arthur Metamorphic Complex consists of the Timbs Group and the adjacent, metamorphosed part of the Oonah Formation. The boundaries are defined by the tectonic feature called the Arthur Lineament (Gee, 1967) shown in 1A.*
Abbreviations: COR = Corinna; SRM = Savage River mine; RR = Rocky River; RD = Reece Dam; A = Alpine locality.

at Savage River was magnesioriebeckite with a substantial actinolite component in solid solution (Green and Spiller, 1977).

Origin of the amphibolite bodies

Amphibolites in the Arthur Metamorphic Complex are interbanded with metasedimentary schist and occur as relatively thin bodies, ranging up to tens of metres in thickness. Spry (1964) suggested that the bodies might, in general, have been intrusions emplaced after F_1 because they display only one foliation rather than the two or more that may be present in the metasedimentary rocks. However textures in an amphibolite in the Nancy Formation (fig. 1) indicate an extrusive rather than an intrusive origin. These textures include tuffaceous texture at 346 300 mE, 5392 200 mN and amygdaloidal texture at 344 100 mE, 5 385 700 mN. Textures in an amphibolite in the Bowry Formation at the Savage River mine have been interpreted as after extrusive pillowed basalt (Spiller, 1974), and the ore association at the mine is regarded as volcanogenic (Coleman, 1975; Weatherstone, 1989).

Except for amphibolite bodies in close proximity to iron ore, the major and trace element composition (e.g. Table 1; Turner and Crawford, 1993) and rare earth element composition (Crawford, 1992) of amphibolites in the Bowry Formation are similar to the composition of amphibolites in the Nancy Formation and Lucy Formation, tholeiitic metabasalt in the nearby Ahrberg Group, and basalt in the more distant Smithton Volcanics and Crimson Creek Formation (fig. 2). Taken together these various basaltic formations are thought to reflect evolving magma generation in a continental margin rift setting.

On the basis of rock composition and sparse primary textural features, it would appear that the amphibolite in the Arthur Metamorphic Complex is derived from volcanic rocks and from intrusions that were penecontemporaneous with volcanism. The structural differences between amphibolite and metasedimentary schist apparently result from mechanical differences, not from late intrusion of the amphibolite protolith.

Mode of occurrence of blue amphibole

In the limited number of rocks in the Bowry Formation that have been found to contain blue amphiboles (Table 2) there is an apparent relationship between the amount of deformation displayed and the mode of occurrence of the blue amphibole. In strongly schistose rocks the blue amphibole occurs as uncommon, relict grains. In more massive rocks, which show less intense preferred orientation of mineral grains, the blue amphibole may be common but is still relict. This trend towards more complete preservation, or less retrogression, of blue amphibole continues in very unusual, massive amphibolite west of Reece Dam, where the blue amphibole shows remarkably little alteration and the rock appears to have very nearly retained its original prograde equilibrium assemblage.

Table 1

Whole rock and trace element analyses of samples from the western (NC513) and eastern (NC516) amphibolite bodies on the track west of Reece Dam. Amphibole is almost entirely of the blue variety.

Sample No.	NC513	NC516
Lab. No.	910530	910531
SiO_2	49.23	50.14
TiO_2	1.69	1.73
Al_2O_3	14.83	14.90
Fe_2O_3	6.38	5.59
FeO	5.69	7.70
MnO	0.16	0.13
MgO	7.11	7.39
CaO	8.46	4.68
Na_2O	1.31	1.10
K_2O	0.28	0.69
P_2O_5	0.19	0.15
SO_3	0.19	0.16
CO_2	0.11	0.15
H_2O^+	4.10	4.91
LOI	(3.65)	(4.27)
Total	99.73	99.42
Ba	44	110
Co	23	28
Cr	79	63
Cu	37	32
Nb	8	9
Ni	91	78
Pb	<10	10
Rb	5	22
Sc	47	48
Sr	310	145
V	340	350
Y	32	24
Zn	67	80
Zr	110	100

Prograde glaucophane amphibolite and its setting

Along a track (fig. 3) trending northwest from the Heemskirk Road near 343 800 mE, 5 379 300 mN, west of Reece Dam, are two intervals of amphibolite in a mostly metasedimentary succession of albite-mica schist and muscovite-quartz schist. The dominant foliation in the schist is a very well developed, very closely spaced crenulation cleavage (S_2). In contrast the amphibolite bodies are relatively massive, particularly the western body (NC493, 513) in which the dominant

Table 2

Location and petrographical summary of the amphibolites

Sample No.	Field No.	AMG (mE)	AMG (mN)	Rock type	Ab	Ep	Chl	Am (B)	Am (G)	Sph	Mt	Hem	Py	Q	Cal	Bt	Mic	Tur
R008503	NC3	343700	5378800	amphibolite	***	***	**	**	***	*	*		*	?		*	*	
R008618	NC118	347000	5379900	mafic schist	***	*	***	*		*	*	*	*	*	*			*
R008993	NC493	343500	5379500	amphibolite	*	***	**	***	**	*	*	*		**			*	
R009012	NC512	343500	5379500	amphibolite	?	***	**	***	*	*	*	*	?	**				
R009013	NC513	343500	5379500	amphibolite														
R009015	NC515	343600	5379500	amphibolite	?	***	**	***		*	*	*	?	**				
R009016	NC516	343600	5379500	amphibolite														
-	G&S7281	350000	5407500	amphibolite	✓	✓	✓	✓	✓	✓	✓		✓	✓				

Abbreviations: Q – quartz; Ab – albite; Ep – epidote; Chl – chlorite; Py – pyrite; Mt – magnetite; Cal – calcite; Am(B) – blue amphibole (prograde); Am(G) – green amphibole (retrograde); Hem – hematite; Tur – tourmaline; Bt – biotite; Mi – white mica; Sph – sphene and leucoxene; *** – >20%; ** – 5–20%; * – <5%?; ✓ – present (abundance undetermined)
G&S7281 – amphibolite from Savage River (Green and Spiller, 1977)

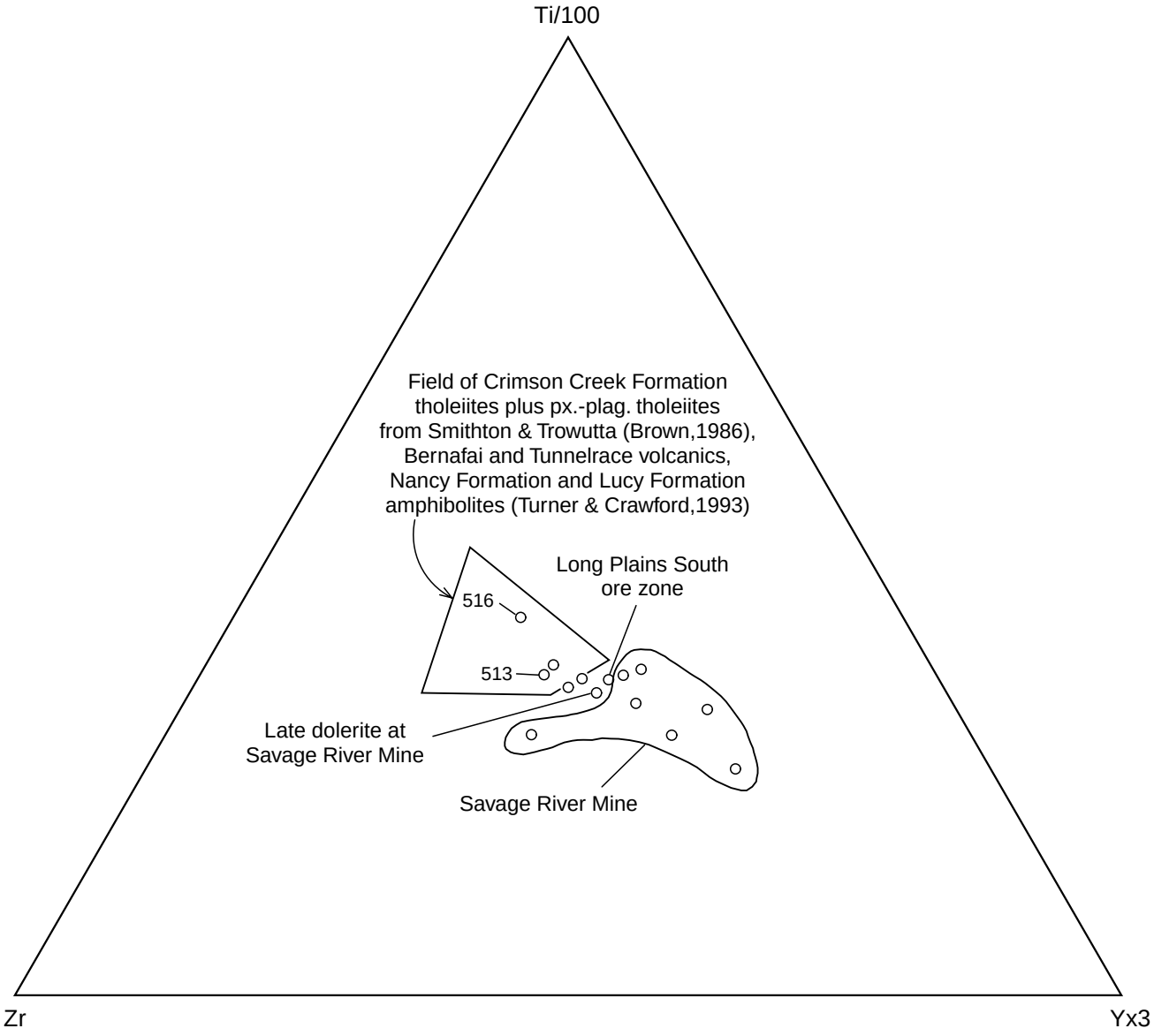

Figure 2

Ti-Zr-Y plot for amphibolites analysed in Table 1 and some other late Proterozoic mafic rocks from the area.

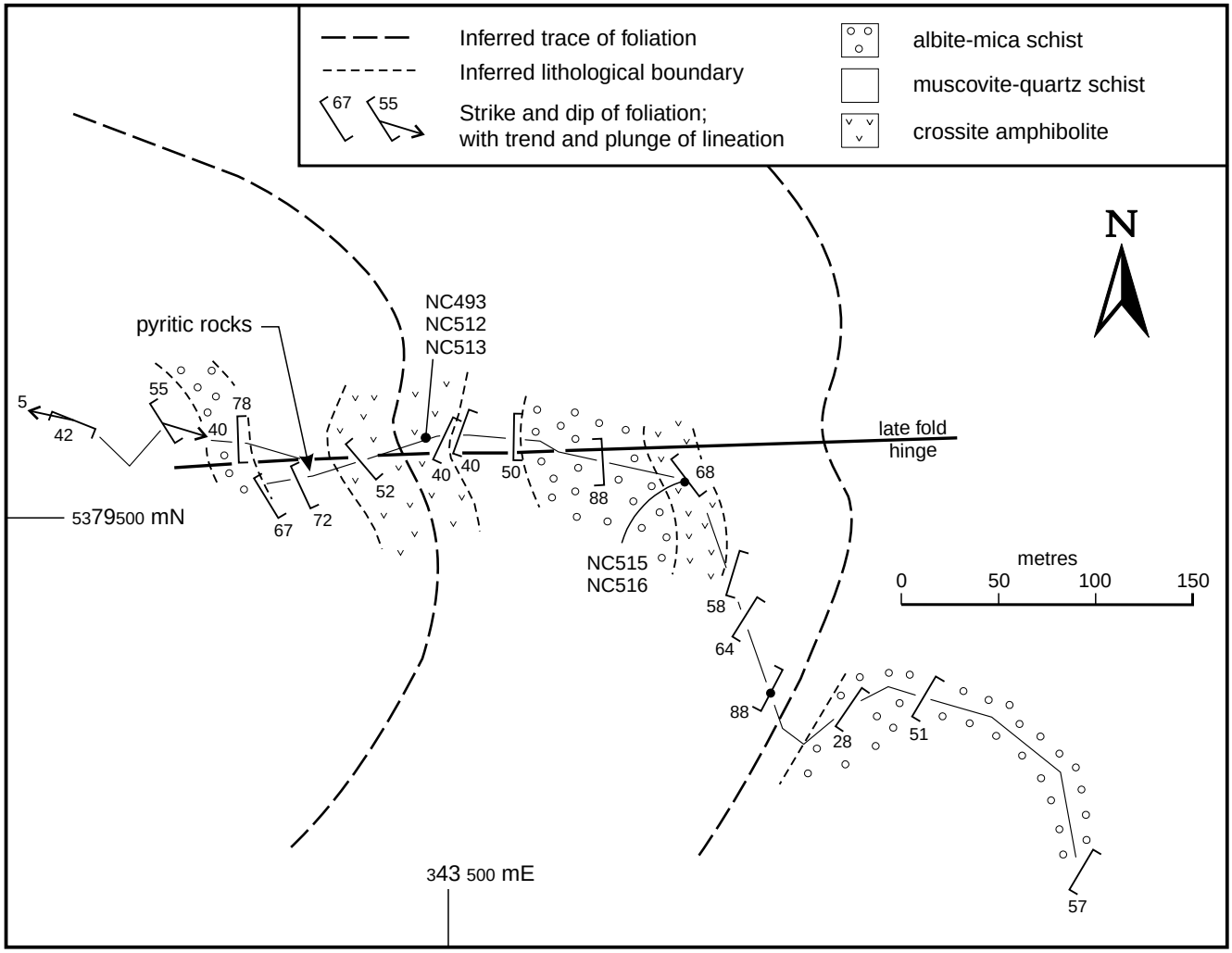

Figure 3

Geology along a track trending northwest from Heemskirk Road near 343 800 mE, 5 379 300 mN, showing sample sites

foliation is crude, scaly and developed only in restricted zones. Foliation in the eastern amphibolite is similarly crude although more pervasive.

Well-crystallised muscovite, which defines the S_1 fabric in the muscovite-quartz schist, is tightly crenulated. Dissolution of quartz in the limbs of the crenulations has concentrated the rotated muscovite, together with fine-grained opaque minerals, into laminae which define the S_2 fabric. In comparison, the microtexture of the albite-mica schist is dominated by albite porphyroblasts in which there is commonly a prominent, straight, internal foliation (S_i) defined by elongate granules of epidote, mica, opaque minerals, greenish brown tourmaline and apatite. The albite grains are surrounded by green biotite, minor muscovite, epidote, chlorite and quartz. These minerals are aligned but have been tightly crenulated to form S_2 which is flattened around the albite grains. S_i (= S_1) in the albite grains may be parallel, oblique or normal to the external S_2 foliation. Shearing along the essentially post-metamorphic S_2 foliation is indicated by partial granulation of some of the common euhedral to subhedral magnetite grains and smearing of the granulated matter along the foliation.

Apart from roughly parallel elongation of very irregularly shaped patches of sphene, there is little microtextural evidence of a foliation in the essentially prograde mineral assemblage in the western amphibolite. In view of the apparently high pressure under which the assemblage crystallised this is unexpected. The porphyroblast relationships in the nearby albite-mica schist indicate that albite, and presumably other peak metamorphic minerals, grew after S_1 (= S_i) had developed. Thus, it appears that the event which produced S_1 in the schists had little effect on the mafic rocks, although they were strongly affected by the post-S_1, pre-S_2 peak metamorphism.

The mineral assemblage in the western amphibolite consists of about 50% by volume of ragged, variably oriented laths of mauve to blue amphibole up to 5 mm long in a matrix of fine-grained epidote, albite and quartz (NC493 in Figure 4). A little green amphibole is present as an alteration product at the margins of a few blue amphibole grains, and patches of chlorite are present within most blue amphibole grains. Whilst the green amphibole marks incipient retrograde metamorphism, the status of the chlorite in the western amphibolite is unclear. It may be part of the prograde assemblage, although the abundance of aligned

chlorite grains with intermixed fine-grained opaque minerals in the more deformed eastern amphibolite strongly indicates that the chlorite in that body is a retrograde product associated with the development of S_2.

Retrograde assemblages

At another locality (343 700 mE; 5 378 800 mN) near Reece Dam there is a boudinaged, medium-grained amphibolite which is fairly massive but which displays strong foliation in restricted zones and around the margins of the body. In the more massive parts of the body (e.g. NC3) there is about 60% by volume of ragged laths of amphibole averaging about 2 mm in length. These amphibole grains are predominantly green but patches of blue to mauve amphibole within the grains make up about one-third of the total amphibole. Well crystallised epidote, together with albite, ?quartz, a little chlorite, common euhedral magnetite and anhedral sphene containing opaque inclusions, make up the remainder of the assemblage. The sphene occurs as ragged, sometimes skeletal grains which are commonly elongate and display a rough alignment that defines a crude foliation.

The mineral assemblage in NC3 apparently represents partial retrogression of a prograde assemblage similar to that in the western amphibolite on the track west of Reece Dam. Fine-grained amphibolite in the same area as NC3 contains strongly aligned, green actinolitic amphibole as its only amphibole mineral. It is therefore considered to have undergone full retrogression from blueschist facies to greenschist facies during the development of S2.

Figure 4

Photomicrograph of blue sodic amphibole partly replaced by green calcic amphibole, plus epidote (granular, yellow, high relief) and albite (colourless, low relief) in NC493. Plane polarised light. Field of view: 1.8 × 1.2 mm. Gl = glaucophane-magnesioriebeckite; Act = actinolite; Ep = epidote; Ab = albite; Sph = sphene; Q = quartz.

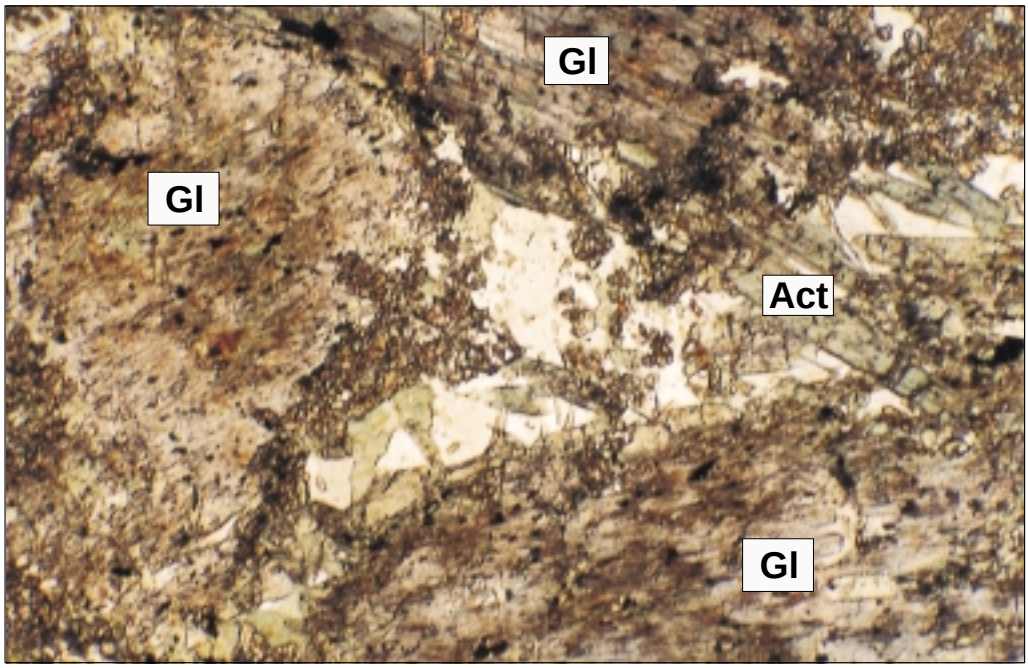

Figure 5

Photomicrograph of blue sodic amphibole partly retrogressed to fine-grained aggregates of green chlorite, colourless albite and dusty calcite, with coarse chlorite, plus epidote (granular, yellow, high relief), albite (colourless, low relief), sphene (dark, high relief) and magnetite (black) in NC118. Plane polarised light. Field of view: 0.7 × 0.5 mm.

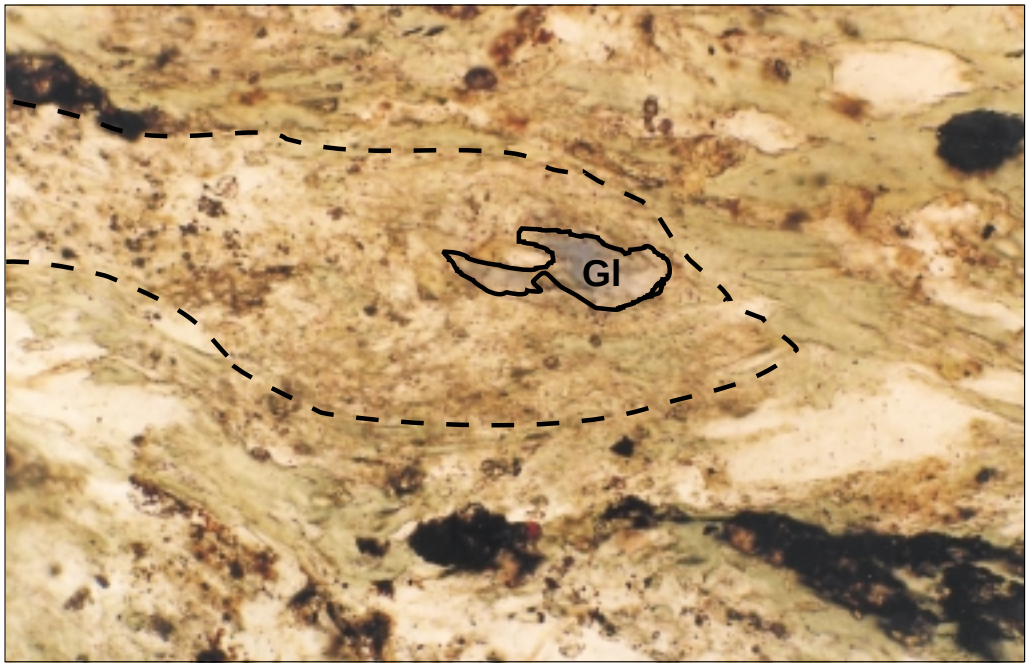

Table 3

Microprobe analyses and structural formulae of amphiboles, Bowry Formation

Sample	G&S7281a	G&S7281b	G&S7281c	NC3	NC3	NC3	NC3	NC3	NC3	NC118	NC118	NC118	NC118	NC493	NC493	NC493	NC493	NC493	NC493
SiO_2	53.66	53.49	53.69	51.33	54.97	56.19	51.13	55.49	55.41	55.00	56.48	55.19	56.13	55.57	55.62	56.45	53.43	51.23	55.02
TiO_2	0.03	0.06	0.06	0.13	0.05	0.07	0.13	0.65	0.10	0.01	0.07	0.05	0.08	0.06	0.19	0.04	0.05	0.10	0.06
Al_2O_3	3.97	3.94	3.41	4.13	1.68	5.46	6.89	3.63	6.48	9.70	10.37	8.41	8.39	6.09	5.19	7.89	4.83	5.71	6.41
Cr_2O_3	0.00	0.00	0.00	0.00	0.00	0.00	0.06	0.07	0.00	0.00	0.01	0.02	0.00	0.10	0.11	0.02	0.03	0.09	0.12
Fe_2O_3	6.87	5.06	3.28	3.20	1.54	4.49	5.14	2.92	4.93	0.00	0.00	0.54	0.40	2.58	4.25	2.54	3.66	4.74	2.44
FeO	14.14	14.74	10.93	12.31	10.31	12.17	10.65	13.20	13.98	15.24	14.43	17.01	16.86	12.44	12.37	11.78	9.98	10.41	12.73
MnO	0.19	0.28	0.28	0.20	0.41	0.31	0.28	0.29	0.15	0.26	0.03	0.12	0.15	0.09	0.17	0.03	0.29	0.17	0.13
MgO	9.67	10.30	14.40	14.08	16.58	10.68	12.08	12.44	8.71	8.21	8.10	8.28	8.17	11.66	11.04	10.65	14.45	13.32	11.54
CaO	2.92	4.99	9.37	10.11	11.93	2.76	7.61	5.20	1.01	1.90	1.21	2.20	1.98	3.31	2.63	1.49	8.84	9.06	3.90
Na_2O	5.82	4.48	2.17	1.41	0.70	5.11	3.41	4.08	6.12	5.29	5.67	5.08	5.31	4.95	5.41	6.07	2.51	2.53	4.60
K_2O	0.02	0.10	0.06	0.62	0.05	0.02	0.16	0.05	0.03	0.05	0.02	0.04	0.00	0.06	0.21	0.01	0.12	0.21	0.07
Total	97.29	97.44	97.65	97.52	98.22	97.26	97.54	98.02	96.92	95.66	96.39	96.94	97.47	96.91	97.19	96.97	98.19	97.57	97.02
Cation distribution																			
Si	7.844	7.815	7.707	7.481	7.810	8.003	7.386	7.920	7.974	7.928	8.000	7.937	8.001	7.925	7.957	7.963	7.597	7.403	7.860
$Al^{(iv)}$	0.156	0.185	0.293	0.519	0.190	0.000	0.614	0.080	0.026	0.072	0.000	0.063	0.000	0.075	0.043	0.037	0.403	0.597	0.140
Sum T	*8.000*	*8.000*	*8.000*	*8.000*	*8.000*	*8.003*	*8.000*	*8.000*	*8.000*	*8.000*	*8.000*	*8.000*	*8.001*	*8.000*	*8.000*	*8.000*	*8.000*	*8.000*	*8.000*
$Al^{(vi)}$	0.528	0.494	0.284	0.191	0.091	0.917	0.559	0.531	1.073	1.576	1.732	1.363	1.410	0.949	0.832	1.275	0.407	0.376	0.940
Ti	0.003	0.007	0.006	0.014	0.005	0.007	0.014	0.070	0.011	0.001	0.007	0.005	0.009	0.006	0.020	0.004	0.005	0.011	0.006
Cr	0.000	0.000	0.000	0.000	0.000	0.000	0.000	0.000	0.000	0.000	0.000	0.000	0.000	0.000	0.000	0.000	0.000	0.000	0.000
Fe^{3+}	0.756	0.557	0.354	0.351	0.164	0.481	0.559	0.314	0.534	0.000	0.000	0.058	0.043	0.277	0.457	0.270	0.392	0.515	0.262
Mg	2.107	2.243	3.081	3.058	3.510	2.267	2.601	2.646	1.868	1.764	1.710	1.775	1.736	2.478	2.354	2.239	3.062	2.869	2.457
Fe^{2+}	1.606	1.699	1.275	1.386	1.224	1.328	1.267	1.439	1.514	1.659	1.551	1.799	1.802	1.290	1.337	1.212	1.134	1.229	1.335
Mn	0.000	0.000	0.000	0.000	0.006	0.000	0.000	0.000	0.000	0.000	0.000	0.000	0.000	0.000	0.000	0.000	0.000	0.000	0.000
Sum C	*5.000*	*5.000*	*5.000*	*5.000*	*5.000*	*5.000*	*5.000*	*5.000*	*5.000*	*5.000*	*5.000*	*5.000*	*5.000*	*5.000*	*5.000*	*5.000*	*5.000*	*5.000*	*5.000*
Fe	0.123	0.102	0.037	0.114	0.000	0.122	0.020	0.137	0.169	0.178	0.158	0.246	0.208	0.194	0.143	0.178	0.052	0.029	0.186
Mn	0.024	0.035	0.034	0.025	0.043	0.037	0.034	0.035	0.018	0.032	0.004	0.015	0.018	0.011	0.021	0.004	0.035	0.021	0.016
Ca	0.457	0.781	1.441	1.579	1.816	0.421	1.178	0.795	0.156	0.293	0.184	0.339	0.302	0.506	0.403	0.225	1.347	1.403	0.597
Na(B)	1.396	1.082	0.488	0.282	0.141	1.411	0.768	1.033	1.657	1.479	1.557	1.400	1.469	1.289	1.433	1.593	0.566	0.547	1.201
Sum B	*2.000*	*2.000*	*2.000*	*2.000*	*2.000*	*1.991*	*2.000*	*2.000*	*2.000*	*1.982*	*1.903*	*2.000*	*1.997*	*2.000*	*2.000*	*2.000*	*2.000*	*2.000*	*2.000*
Na(A)	0.254	0.187	0.116	0.116	0.052	0.000	0.187	0.096	0.051	0.000	0.000	0.017	0.000	0.080	0.068	0.067	0.126	0.162	0.073
K	0.004	0.019	0.011	0.115	0.009	0.004	0.030	0.009	0.006	0.009	0.004	0.007	0.000	0.011	0.038	0.002	0.022	0.039	0.013
Sum A	*0.258*	*0.206*	*0.127*	*0.231*	*0.061*	*0.004*	*0.217*	*0.105*	*0.057*	*0.009*	*0.004*	*0.024*	*0.000*	*0.091*	*0.106*	*0.069*	*0.148*	*0.201*	*0.086*
Tot. cat.	15.258	15.206	15.127	15.231	15.061	14.998	15.217	15.105	15.057	14.991	14.907	15.024	14.998	15.091	15.106	15.069	15.148	15.201	15.086
Mg/Mg+Fe	0.567	0.569	0.707	0.688	0.741	0.631	0.672	0.648	0.552	0.515	0.524	0.497	0.491	0.658	0.638	0.649	0.730	0.700	0.648
(Ca/Ca+Na)B	0.247	0.419	0.747	0.848	0.928	0.230	0.605	0.435	0.086	0.165	0.106	0.195	0.171	0.282	0.219	0.124	0.704	0.719	0.332
Classification	win	win	act	mg-hbd	act	win	bar	win	gl	win	gl	fe-win	fe-win	win	win	gl	win	bar	win

Cation distributions and Fe^{3+} calculated using average of minimum and maximum constraints (Holland and Blundy, 1994).
See Table 6 for abbreviations.

Table 4

Microprobe analyses of chlorites coexisting with blue amphiboles, Bowry Formation

Anal. No.	NC493	NC493	NC3	NC3	Nc118	Nc118	Nc118
Phase	Chl#1	Chl#2	Chl#1	Chl#2	Chl#1	Chl#2	Chl#3
SiO_2	27.22	27.81	26.94	27.70	25.83	26.16	26.71
TiO_2	0.02	0.00	0.03	0.19	0.06	0.07	0.03
Al_2O_3	18.94	18.88	18.81	17.30	20.46	20.41	19.96
Cr_2O_3	0.33	0.16	0.09	0.14	0.05	0.05	0.00
MgO	21.11	21.88	19.83	19.38	17.60	16.74	17.34
CaO	0.03	0.01	0.00	0.32	0.05	0.04	0.00
MnO	0.18	0.00	0.22	0.19	0.07	0.12	0.18
FeO	18.67	17.98	21.37	21.68	23.63	24.04	24.03
Total	86.53	86.73	87.29	86.90	87.75	87.63	88.25
Atomic ratios (28 Oxygen)							
Si	5.620	5.691	5.592	5.790	5.395	5.476	5.547
$Al^{(iv)}$	2.380	2.309	2.408	2.210	2.605	2.524	2.453
$Al^{(tot)}$	4.607	4.551	4.601	4.261	5.034	5.034	4.884
Ti	0.004	0.000	0.005	0.030	0.009	0.011	0.005
$Al^{(vi)}$	2.228	2.242	2.193	2.051	2.429	2.510	2.431
Cr	0.054	0.025	0.014	0.024	0.008	0.009	0.000
Mg	6.496	6.672	6.135	6.037	5.478	5.223	5.366
Ca	0.007	0.003	0.000	0.072	0.012	0.008	0.000
Mn	0.031	0.000	0.039	0.033	0.012	0.021	0.032
Fe	3.225	3.076	3.710	3.791	4.127	4.209	4.173
Total	20.045	20.017	20.096	20.038	20.075	19.992	20.006
Mg/Mg+Fe	0.668	0.684	0.623	0.614	0.570	0.554	0.563

Mafic schist is interbanded with magnesite and dolomite about 20 km north of Reece Dam at Main Creek. This schist (e.g. NC118) consists mainly of chlorite, carbonate, albite, ?quartz, minor epidote, euhedral magnetite, anhedral opaque minerals and sphene. Preferred orientation of chlorite grains, seams of opaque minerals, and elongate carbonate patches define the strong schistosity which is deflected around sparse, relict grains of blue to mauve amphibole and rare, relict, pale pinkish brown to olive green tourmaline grains. The blue amphibole grains are stubby laths of variable orientation that show partial alteration to carbonate, chlorite and albite (fig. 5).

As is the case in the amphibolite bodies near Reece Dam, there is only one foliation evident in the mafic schist at Main Creek and it post-dates the crystallisation of blue amphibole. Evidence of shearing is provided by seams of finely granular opaque minerals smeared along the foliation. Retrogressive metamorphism, associated with foliation development and shearing and combined with earlier carbonate replacement, produced the Main Creek mafic schist, probably from an original blue amphibole-bearing amphibolite.

Analytical procedures and formulae calculation

The amphiboles and associated minerals were analysed with a Cameca SX-50 electron microprobe, using WDS spectrometers at 15 kV, at the University of Tasmania; the results are given in Tables 3–5. The amphibole formulae and Fe^{3+} were determined from the weight % oxides using the methods of Holland and Blundy (1994) and Schumacher (1997). The amphibole nomenclature is that of Leake *et al*. (1997).

To determine the mineral species the cation distributions were calculated in accord with the standard amphibole formula of $AB_2C_5{}^{vi}T_8{}^{iv}O_{22}(OH,O,Cl,F)_2$. The FeO/Fe_2O_3 ratios were not determined separately but were calculated by crystal chemical considerations and the average of minimum and maximum constraints (Holland and Blundy, 1994 Schumacher, 1997). These methods provide a reasonable approximation in most cases.

Results

Analytical data for the sodic amphiboles (fig. 6) show that they all plot as glaucophane. Note that only true sodic amphiboles, with $Na^B > 1.5$ (Leake *et al*., 1997), are included in Figure 6, and none of the analyses of Green and Spiller (1977) fall within this field. The sodic amphiboles are all blue coloured and appear to be texturally prograde. Data for green amphiboles (fig. 7) show a range of sodic-calcic to calcic amphibole species including barroisite, winchite, ferrowinchite, magnesiohornblende and actinolite, all texturally retrograde.

The minerals in the equigranular amphibolite NC493, from west of Reece Dam, consist of glaucophane-winchite, epidote, albite, chlorite, sphene and iron oxides. This apparently prograde assemblage supports the use of the following reaction as a geobarometer (from Brown, 1977).

Ca-amphibole + chlorite + albite + iron oxide
→ Na-amphibole + epidote + water

Pressures of up to about 650–700 MPa are indicated by this method (fig. 7). Samples NC3 and NC118, despite being more retrogressed, give similar results.

Similar pressures of around 700 MPa are indicated by the Maruyama *et al*. (1986) plot (fig. 8) for the sodic amphiboles and co-existing chlorites (Table 4). Some uncertainty is attached to this presentation because of

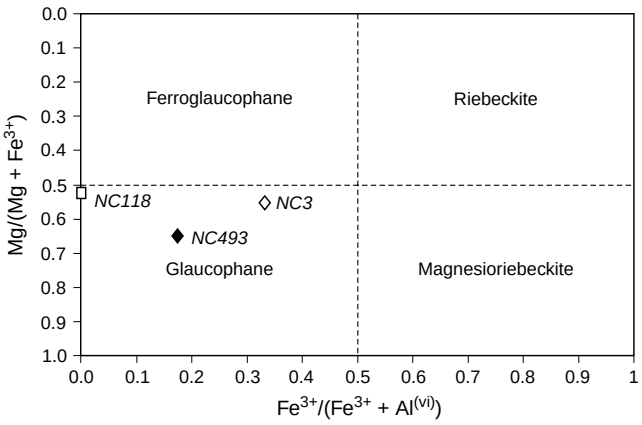

Figure 6

Sodic amphiboles (with Na^B >1.5), Bowry Formation: Mg/ (Mg+Fe^{2+}) vs Fe^{3+}/(Fe^{3+}+Al^{vi}), with compositional fields from Leake et al. *(1997).*

Table 5

Microprobe analyses of feldspars, epidotes, calcites coexisting with blue amphiboles, Bowry Formation

	Feldspars			Epidotes						Carbonates		
Sample	NC118	NC118	NC493	NC3	NC3	NC118	NC118	NC493	NC493	NC118	NC118	NC118
spot	3a-ab1	3b-ab2	ab1	1a-ep1	2d-ep1	3b-ep1	39-ep2	ep1	ep2	3b-cal1	40-cal2	41-cal3
SiO_2	66.30	68.01	69.54	36.02	36.16	36.99	39.96	37.31	37.57			
TiO_2	0.00	0.00	0.00	0.11	0.13	0.09	0.12	0.01	0.07			
Al_2O_3	18.99	19.16	19.66	20.98	21.68	23.14	24.31	21.98	22.21			
Cr_2O_3	0.02	0.01	0.01	0.10	0.09	0.00	0.00	0.01	0.00			
FeO	0.09	0.12	0.28	13.95	13.31	12.13	9.51	14.12	13.60	1.35	1.80	1.34
MnO	0.01	0.00	0.02	0.38	0.48	0.23	0.16	0.17	0.21	0.74	0.82	0.79
MgO	0.00	0.00	0.00	0.00	0.00	0.02	0.64	0.00	0.00	0.82	0.88	0.82
CaO	0.20	0.46	0.06	23.06	23.54	23.42	18.51	23.50	23.99	53.51	55.00	53.16
Na_2O	10.41	11.04	11.05	0.08	0.01	0.08	0.00	0.07	0.02			
K_2O	0.04	0.01	0.02	0.02	0.00	0.01	1.98	0.00	0.02			
Total	96.06	98.98	100.67	95.01	95.75	96.52	95.47	97.57	98.19	56.42	58.50	56.10
Atomic ratios												
Sum:	To 8 oxygens			To 8 cations						To 1 cation		
Si	3.004	3.003	3.009	2.947	2.932	2.960	3.194	2.970	2.972	0.000	0.000	0.000
Ti	0.000	0.000	0.000	0.007	0.008	0.005	0.007	0.000	0.004	0.000	0.000	0.000
Al	1.014	0.997	1.002	2.023	2.072	2.182	2.290	2.062	2.070	0.000	0.000	0.000
Cr	0.001	0.000	0.000	0.006	0.006	0.000	0.000	0.001	0.000	0.000	0.000	0.000
Mg	0.000	0.000	0.000	0.000	0.000	0.002	0.076	0.000	0.000	0.020	0.021	0.020
Ca	0.010	0.022	0.003	2.022	2.046	2.008	1.585	2.005	2.034	0.951	0.944	0.950
Mn	0.000	0.000	0.001	0.027	0.033	0.015	0.011	0.012	0.014	0.010	0.011	0.011
Fe	0.003	0.005	0.010	0.954	0.902	0.812	0.636	0.940	0.900	0.019	0.024	0.019
Na	0.915	0.945	0.927	0.012	0.002	0.013	0.000	0.010	0.003	0.000	0.000	0.000
K	0.002	0.001	0.001	0.002	0.000	0.001	0.201	0.000	0.002	0.000	0.000	0.000
Total	4.948	4.972	4.954	8.000	8.000	8.000	8.000	8.000	8.000	1.000	1.000	1.000
sum Si+Al	4.017	3.999	4.011	4.970	5.004	5.142	5.484	5.032	5.042			
sum Alk	0.926	0.967	0.931									
%An	1.040	2.252	0.291									

Table 6

Mineral reactions shown in Figure 9

No.	Reaction	Reference
1.	Act + Ab + Mt → Ep + Crossite	Ibarguchi and Dallmeyer, 1991
2.	Glaucophane experimental low P stability limits (→ smectite)	Maresch, 1977
3.	Barroisite low P stability limit	Ernst, 1979
4.	Cz + Chl + Tr + Q → Hbd + w	Liou *et al*., 1987
5.	Pm + Chl + Q → Cz + Tr + w	Liou *et al*., 1987
6.	Lw + Pm → Cz + Chl + Q + w	Liou *et al*., 1987
7.	Lw + Gl → Ab + Pm + Chl + Q + w	Liou *et al*., 1987
8.	Lw + Pm + Ab → Cz + Gl + Q + w	Liou *et al*., 1987
9.	Lw + Gl → Ab + Cz + Chl + Q + w	Liou *et al*., 1987
10.	Pm + Chl + Ab → Cz + Gl + w	Liou *et al*., 1987
11.	Pm + Gl + Q → Cz + Tr + Ab + w	Liou *et al*., 1987
12.	Tr + chl + Ab → Gl + Cz + Q + w	Maruyama *et al*., 1986

Abbreviations

Act:	actinolite	Hbd:	hornblende
Ab:	albite	Lw:	lawsonite
Bar:	barroisite	Mt:	magnetite
Chl:	chlorite	Pm:	pumellyite
Cz:	clinozoisite	Q:	quartz
Gl:	glaucophane	Tr:	tremolite
Gl-x:	glaucophane (experimental)	w:	water
win:	winchite	Fe-win:	ferrowinchite
mg-hbd:	magnesiohornblende		

the need to distinguish between prograde and retrograde chlorite. However the selected chlorites have a low compositional range, and at high P their compositions have little effect on the indicated pressure.

El-Shazly (1994) used the methods of Brown (1977) and Maruyama *et al. (1986*) to estimate pressures in glaucophane-bearing metabasites, but considered the results suspect in the northeast Oman case as the equilibrium assemblage (Na-amphibole-epidote-albite-chlorite-Fe oxide) may not have been present at peak pressure. Sample NC493 does contain the required assemblage, which appears texturally prograde, thus justifying the use of the methods.

A common associate of blue amphibole, lawsonite, has not been identified in the rocks described here. This is probably because the thermal gradient was too high. Pure lawsonite, below about 800 MPa, becomes thermodynamically unstable above about 260°C, being replaced by epidote and other minerals (fig. 9).

Chlorite compositions, especially Al contents, are known to be largely temperature dependant in metamorphic rocks (Laird, 1988). A chlorite geothermometer has been devised empirically from low pressure hydrothermal systems on this basis

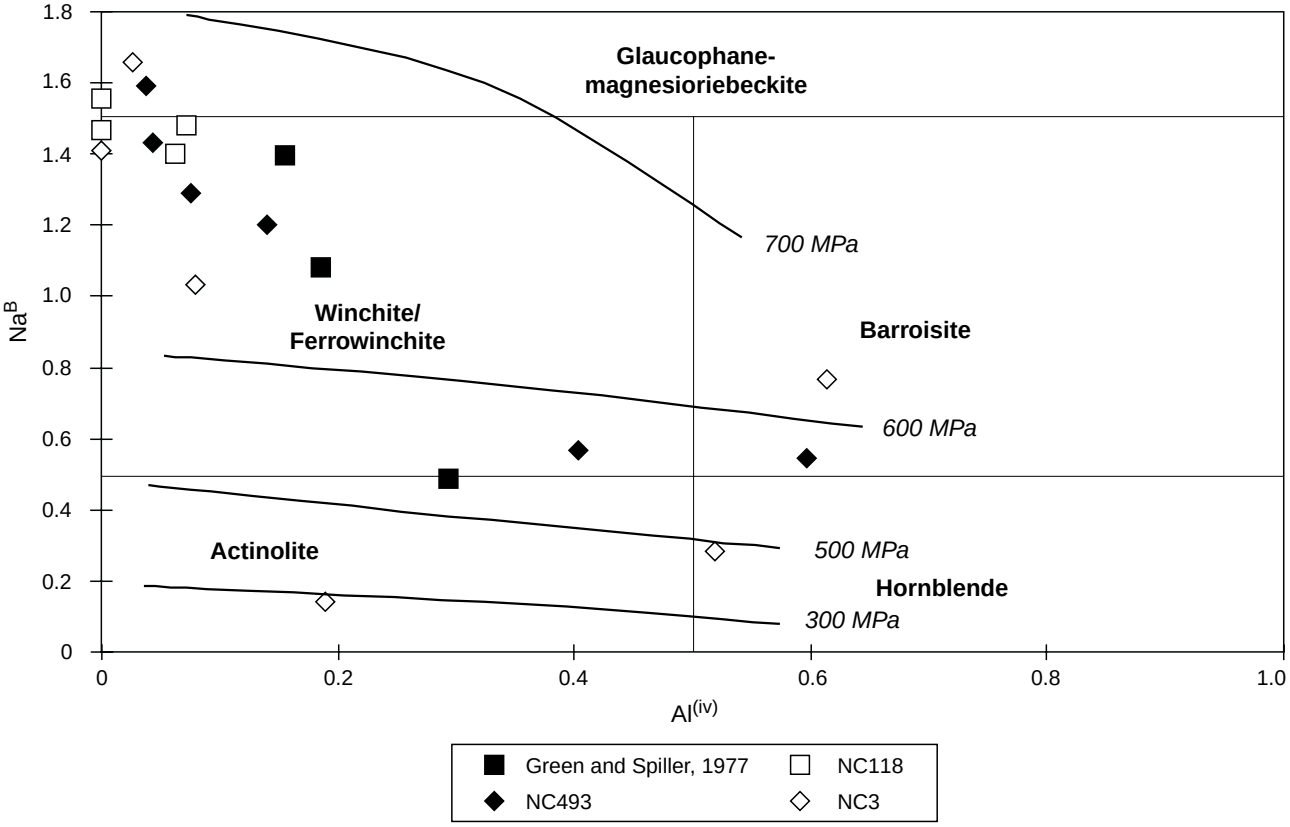

Figure 7

Amphiboles, Bowry Formation: Na^{M4} vs Al^{iv}, with compositional fields from Leake et al.*, 1997. Isobars shown from Brown (1977).*

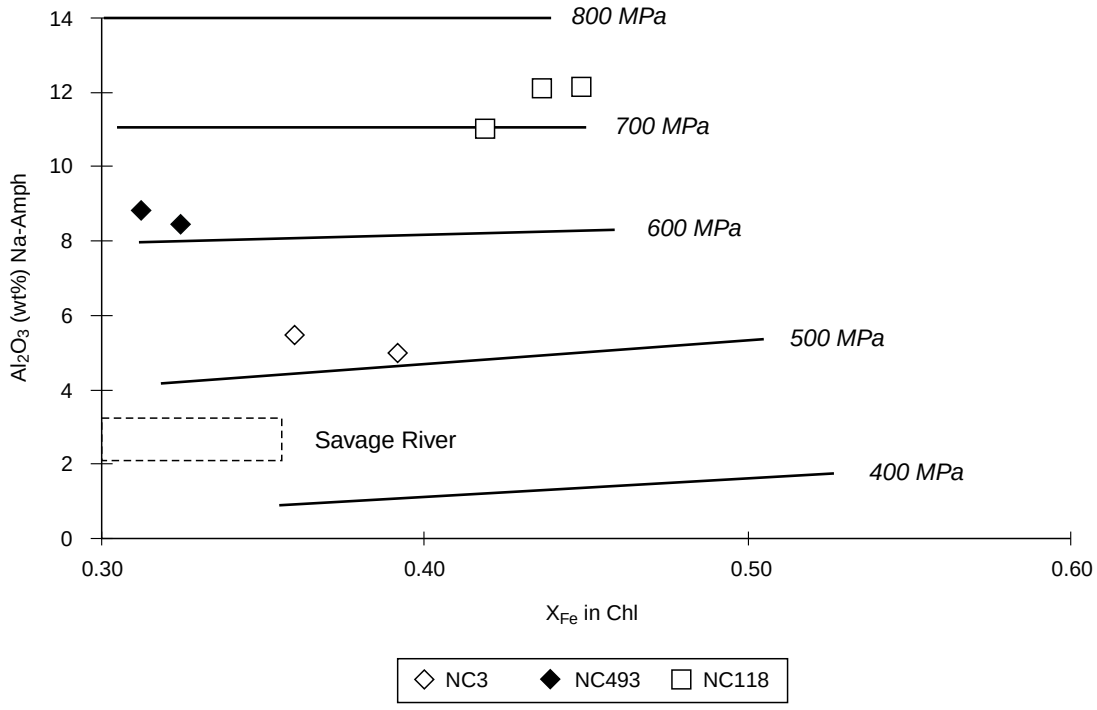

Figure 8

Amphiboles, Bowry Formation: wt% Al_2O_3 in amphiboles vs X_{Fe} in chlorites, showing isobars from Maruyama et al. *(1986).*

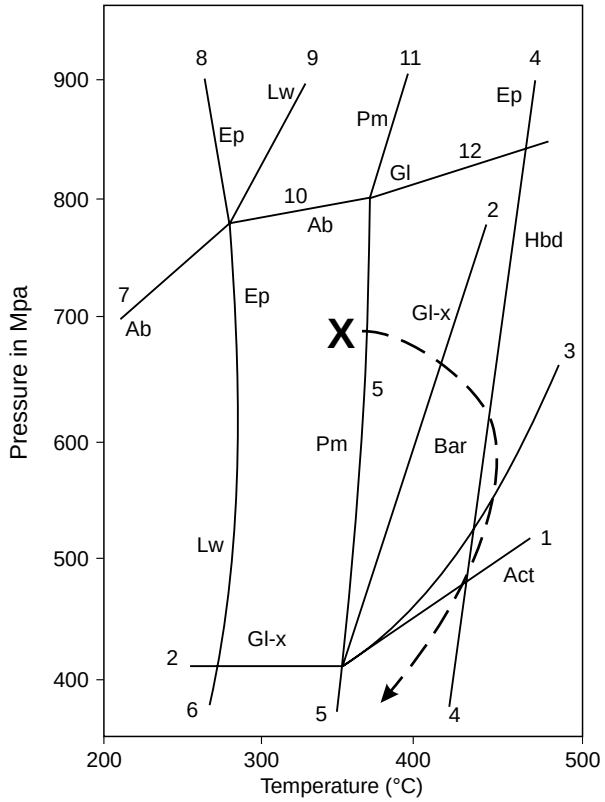

Figure 9

P-T diagram, showing a petrogenetic grid based on pure systems for various medium to high-pressure metamorphic facies and their basaltic assemblages. See Table 6 for reactions and abbreviations. The peak metamorphic conditions determined are represented by X. A retrograde path that is consistent with the observed minerals is shown.

(Cathelineau and Nieva, 1985; Cathelineau, 1988). Despite being based on shallow hydrothermal systems, this gives sensible results where tested in both pelites and hydrothermal veins formed in regionally metamorphosed rocks (Cathelineau, 1988; Bevins *et al*., 1991; Taheri and Bottrill, 1994). The method assumes an open chemical system (Cathelineau, 1988). Applying the chlorite geothermometer to the amphibolites in this study gives a range of temperatures from 280–345°C, although these may be somewhat retrograde temperatures.

The equigranular texture of the prograde glaucophane-magnesioriebeckite assemblage in the amphibolite west of Reece Dam suggests that blueschist facies metamorphism took place under static conditions, presumably in a structurally protected part of the subducted mass, probably with the amphibole minerals replacing pyroxene in gabbro. Although some hornblende textures are non-schistose, it is likely that this mineral reflects amphibolite facies retrogression during emplacement.

Non-schistose textures involving hornblende suggest that this mineral also crystallised before the onset of structural emplacement. It is likely that the different periods of metamorphic conditions that are represented by hornblende and the blue amphiboles were of similar age, that is, about 510 Ma minimum. The subducted rocks possibly experienced some heating prior to structural emplacement, with consequent hornblende crystallisation, but did not fully equilibrate. During emplacement the metagabbro bodies were largely recrystallised to schistose, greenschist facies amphibolite.

Figure 10 illustrates an empirical relationship between minimum $(Fe^{3+}/Fe^{3+}+Al)$ and metamorphic grade, and shows compositional similarities between the amphiboles at Corinna and in the Sambagawa and Oman terrains.

Terrain comparison

Marked similarities between the Arthur Lineament and the Japanese Sambagawa Belt (Wallis and Banno, 1990) have been noted by Turner *et al*. (1992). The similarities include:

- The Arthur Lineament and the Sambagawa Belt are both narrow, linear features containing high-pressure metamorphic assemblages.
- Compositional parameters of blue amphiboles from each terrain are remarkably similar (fig. 10).
- In each terrain the protolith succession comprises thick, continentally-derived, clastic sediments with rift-related basaltic volcanic rocks.
- Mineralisation at the Alpine locality (fig. 1) resembles the Besshi-style, pyrite-rich copper deposits of the Sambagawa Belt (Fox, 1984) in terms of major mineralogy and regional setting.

The above listing shows enough features in common between the two terrains to warrant a more exhaustive comparison. Such a comparison is being currently undertaken and has shown dissimilarities as well as similarities. Dissimilarities include:

- A more alkaline composition for basaltic rocks in the Sambagawa Belt.
- Much more extensive development and preservation of high-pressure and temperature mineral assemblages in the Sambagawa Belt. In the Arthur Lineament these assemblages are only known in the Bowry Formation, where their sparse occurrence indicates near-pervasive retrograde metamorphism.
- Garnet has been recognised by these authors in metasedimentary rocks in the Arthur Lineament. Garnet represents an intermediate level of metamorphism, at higher temperature, in the metasedimentary rocks of the Sambagawa Belt (fig. 9), so perhaps only the lower (deeper) zones of Sambagawa metamorphism are represented in the Arthur Lineament. Blue amphibole assemblages in the mafic rocks of the Arthur Lineament are consistent with the upper chlorite zone of

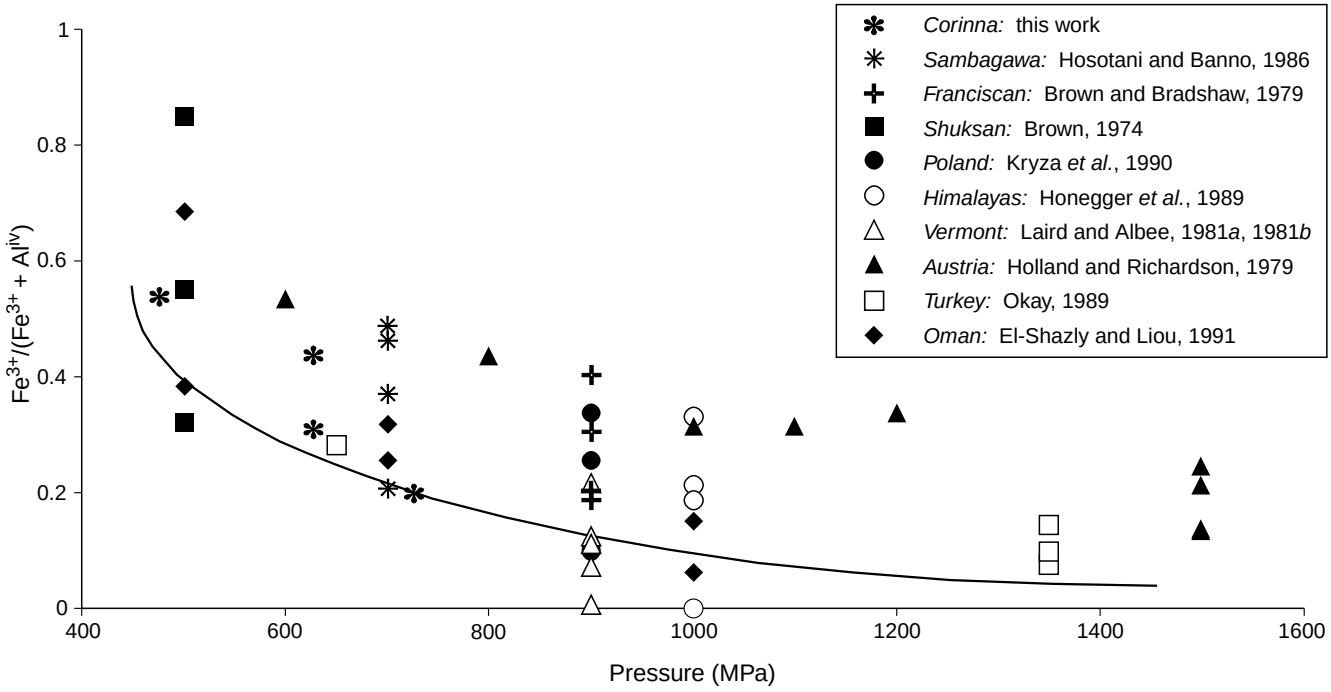

Figure 10

$Fe^{3+}/(Fe^{3+}+Al^{vi})$ values for amphiboles from different high-P terrains, with an approximate line of best fit.

Sambagawa-type metamorphism, just below the garnet zone. Some mafic assemblages in which prograde hornblende has been optically identified may be of higher temperature (fig. 9). Further microprobe work is necessary to precisely determine the composition and petrogenesis of the green-brown amphiboles identified as hornblende in these rocks.

- The Sambagawa Belt is a younger terrain than the Arthur Lineament in terms of protolith age and age of metamorphism. Respectively, the protolith age and age of metamorphism are Late Proterozoic (?600 Ma) and Cambrian (?510 Ma minimum: Turner *et al*., 1992) for the Arthur Lineament, compared with Late Palaeozoic and Cretaceous for the Sambagawa Belt (Wallis and Banno, 1990).

Conclusions

Sparsely preserved, relict, prograde metamorphic blue amphiboles in the Bowry Formation of the Arthur Metamorphic Complex have glaucophane-winchite compositions. The presence of these blue amphiboles suggest that the rocks were subjected to pressures of around 7 kb (700 MPa), possibly corresponding to a depth of burial of the order of 25 kilometres. Such a depth of burial is probably only achievable in a crustal collision zone.

There are marked similarities between the Arthur Lineament, that is, the tectonic feature which contains the Arthur Metamorphic Complex, and the Japanese Sambagawa Belt. However, it appears that only the lower grade Sambagawan metamorphic zones may be represented in the Arthur Lineament.

References

BEVINS, R. E.; ROBINSON, D.; ROWBOTHAM, G. 1991. Compositional variations in mafic phyllosilicates from regional low-grade metabasites and application of the chlorite geothermometer. *Journal Metamorphic Geology* 9:711–721.

BROWN, A. V. 1986. Geology of the Dundas–Mt Lindsay–Mt Youngbuck region. *Bulletin Geological Survey Tasmania* 62.

BROWN, E. H. 1974. Comparison of the mineralogy and phase relations of blueschists from the North Cascades, Washington, and greenschists from Otago, New Zealand. *Bulletin Geological Society America* 85:333–344.

BROWN, E. H. 1977. The crossite content of Ca-amphibole as a guide to pressure of metamorphism. *Journal of Petrology* 18:53–72.

BROWN, E. H.; BRADSHAW, J. Y. 1979. Phase relations of pyroxene and amphibole in greenstone, blueschist and eclogite of the Franciscan Complex, California. *Contributions to Mineralogy and Petrology* 71:67–83.

CATHELINEAU, M. 1988. Cation site occupancy in chlorites and illites as a function of temperature. *Clay Minerals* 23:471–485.

CATHELINEAU, M.; NIEVA, D. 1985. A chlorite solid solution geothermometer; the Los Azufres (Mexico) geothermal system. *Contributions to Mineralogy and Petrology* 91:235–244.

COLEMAN, R. J. 1975. Savage River magnetite deposits, *in:* KNIGHT, C. L. (ed.). Economic geology of Australia and Papua New Guinea. I. Metals. *Monograph Serial Australasian Institute of Mining and Metallurgy* 5:598–604.

CRAWFORD, A. J. 1992. Geochemistry and implications of mafic metavolcanics in the Corinna–Savage River area, *in:* TURNER, N. J. (ed.). Corinna 1:50 000 geological map. Field guide to selected rock exposures. *Report Department of Mines Tasmania* 1992/06:27–37.

EL-SHAZLY, A. K. 1994. Petrology of lawsonite-, pumpellyite- and sodic amphibole-bearing metabasites from north-east Oman. *Journal Metamorphic Petrology* 12:23–48.

EL-SHAZLY, A. K.; LIOU, J. G. 1991. Glaucophane chloritoid-bearing assemblages from NE Oman: petrologic significance and a petrogenetic grid for high P metapelites. *Contributions to Mineralogy and Petrology* 107:180–201.

ERNST, W. G. 1979. Coexisting sodic and calcic amphiboles from high-pressure metamorphic belts and the stability of barroisitic amphibole. *Mineralogical Magazine* 43:269–278.

FOX, J. S. 1984. Besshi-type volcanogenic sulphide deposits; a review. *Bulletin Canadian Institute of Mining* 77:57–68.

GEE, R. D. 1967. The Proterozoic rocks of the Rocky Cape geanticline, *in: The geology of Western Tasmania – A Symposium*. University of Tasmania : Hobart.

GEE, R. D. 1989. Precambrian—North coastal section, *in:* BURRETT, C. F.; MARTIN, E. L. (ed.). The geology and mineral resources of Tasmania. *Special Publication Geological Society Australia* 15:11–14.

GREEN, T. H.; SPILLER, A. R. 1977. Blue amphibole from Precambrian metabasalts, Savage River, Tasmania. *American Mineralogist* 62:164–166.

HOLLAND, T. J. B.; BLUNDY, J. 1994. Non-ideal interactions in calcic amphiboles and their bearing on amphibole plagioclase thermometry. *Contributions to Mineralogy and Petrology* 116:433–447.

HOLLAND, T. J. B.; RICHARDSON, S. W. 1979. Amphibole zonation in metabasites as a guide to the evolution of metamorphic conditions. *Contributions to Mineralogy and Petrology* 70:143–148.

HONEGGER, K.; LEFORT, P.; MASCLE, G.; ZIMMERMANN, J. L. 1989. The blueschists along the Indus Suture Zone in Ladakh, northwestern Himalayas. *Journal Metamorphic Geology* 7:57–72.

HOSOTANI, H.; BANNO, S. 1986. Amphibole composition as an indicator of subtle grade variation in epidote-glaucophane schists. *Journal Metamorphic Geology* 4:23–35.

IBARGUCHI, J. I. G.; DALLMEYER, R. D. 1991. Hercynian blueschist metamorphism in North Portugal — tectonothermal implications. *Journal Metamorphic Geology* 9:539–549.

KRYZA, R.; MUSZYNSKI, A.; VIELZEUF, D. 1990. Glaucophane-bearing assemblages overprinted by greenschist-facies metamorphism in the Variscan Kaczawa complex, Sudetes, Poland. *Journal Metamorphic Geology* 8:345–355.

LAIRD, J. 1988. Chlorites: metamorphic petrology, *in* BAILEY, S. W. Hydrous phyllosilicates. *Reviews in Mineralogy* 19:405–453. Mineralogical Society of America.

LAIRD, J.; ALBEE, A. L. 1981*a*. High-pressure metamorphism in mafic schist from Northern Vermont. *American Journal of Science* 281:97–126.

LAIRD, J.; ALBEE, A. L. 1981*b*. Pressure, temperature, and time indicators in mafic schist; their application to reconstructing the polymetamorpic history of Vermont. *American Journal of Science* 281:127-175.

LEAKE, B. E. 1978. Nomenclature of amphiboles. *Canadian Mineralogist* 16:501–520.

LEAKE, B. E.; WOOLLEY, A. R. ; ARPS, C. E. S.; BIRCH, W. D.; *and others*. 1997. Nomenclature of amphiboles: Report of the Subcommittee on Amphiboles of the International Mineralogical Association Commission on New Minerals and Mineral Names. *Mineralogical Magazine* 405:295–321.

LIOU, J. G.; MARUYAMA, S.; *et al*. 1987. Very low grade metamorphism of volcanic and volcaniclastic rocks — mineral assemblages and mineral facies, *in:* FREY, M. (ed.). *Low temperature metamorphism*. 59-113. Blackie : Glasgow.

MARUYAMA, S.; CHO, M.; LIOU, J. G. 1986. Experimental investigations of blueschist-greenschist transition equilibria: pressure dependence of Al_2O_3 contents in sodic amphiboles; a new geobarometer. *Memoir Geological Society America* 164:1–16.

MARESCH, W. V. 1977. Experimental studies on glaucophane: an analysis of present knowledge. *Tectonophysics* 43:109–125.

OKAY, A. I. 1989. An exotic eclogite/blueschist slice in a Barrovian-style metamorphic terrain, Alanya Nappes, Southern Turkey. *Journal of Petrology* 30:107–132.

ROBINSON, P.; SPEAR, F. S.; SCHUMACHER, J. C.; LAIRD, J.; KLEIN, C.; EVANS, B. W.; DOOLAN, B. L. 1982. Phase relations of metamorphic amphiboles: natural occurrence and theory, *in:* VEBLEN, D. R.; RIBBE, P. H. (ed.). Amphiboles: petrology and phase relations. *Reviews in Mineralogy* 9B:3–8. Mineralogical Society of America.

SCHUMACHER, J. C. 1997. The estimation of ferric iron in electron microprobe analyses. Appendix 2 *in:* LEAKE, B. E.; WOOLLEY, A. R. ; ARPS, C. E. S.; BIRCH, W. D.; *and others*. Nomenclature of amphiboles: Report of the Subcommittee on Amphiboles of the International Mineralogical Association Commission on New Minerals and Mineral Names. *Mineralogical Magazine* 405:312–321.

SMELIK, E. A.; VEBLEN, D. R. 1991. Exsolution of cummingtonite from glaucophane: a new orientation for exsolution lamellae in clinoamphiboles. *American Mineralogist* 76:971–984.

SPILLER, A. R. 1974. *The petrology of the Savage River iron ore deposit, Tasmania*. B.A. (Hons) thesis, Macquarie University.

SPRY, A. 1964. Precambrian rocks of Tasmania, Part VI, the Zeehan–Corinna area. *Papers Proceedings Royal Society Tasmania*. 98:23–48.

TAHERI, J.; BOTTRILL, R. S. 1994. A study of the nature and origin of gold mineralisation, Mangana–Forester area, northeast Tasmania. *Report Department of Mines Tasmania* 1994/05.

TURNER, N. J. 1993. K-Ar geochronology in the Arthur Metamorphic Complex, Ahrberg Group and Oonah Formation, Corinna district. *Report Mineral Resources Tasmania* 1993/27.

TURNER, N. J.; BOTTRILL, R. S.; CRAWFORD, A. J.; VILLA, I. 1992. Geology and prospectivity of the Arthur Mobile Belt. *Bulletin Geological Survey Tasmania* 70:227–233.

TURNER, N. J.; BROWN, A. V.; MCCLENAGHAN, M. P.; SOETRISNO, Ir. 1991. Geological Atlas 1:50 000 Series. Sheet 43 (7914N). Corinna. *Department of Resources and Energy, Tasmania*.

TURNER, N. J.; CRAWFORD, A. J. 1993. General features and chemical analyses of mafic and other rocks, Corinna geological map quadrangle. *Report Mineral Resources Tasmania* 1993/23.

WALLIS, S.; BANNO, S. 1990. The Sambagawa belt; trends in research. *Journal Metamorphic Geology* 8:393–399.

WEATHERSTONE, N. 1989. Savage River iron ore deposits, in:. Geology and Mineral Resources of Tasmania, *in:* BURRETT, C. F.; MARTIN, E. L. (ed.). The geology and mineral resources of Tasmania. *Special Publication Geological Society Australia* 15:23–24.

[31 July 2000]